

Disaster Assessment from Satellite Imagery by Analysing Topographical Features Using Deep Learning

Saramsha Dotel
Institute of Engineering,
Tribhuvan University
Pulchowk, Lalitpur, Nepal
072bct534dotel@pcampus.edu.np

Avishekh Shrestha
Institute of Engineering,
Tribhuvan University
Pulchowk, Lalitpur, Nepal
072bct507.avishekh@pcampus.edu.np

Anish Bhusal
Institute of Engineering,
Tribhuvan University
Pulchowk, Lalitpur, Nepal
072bct505.anish@pcampus.edu.np

Ramesh Pathak
Institute of Engineering,
Tribhuvan University
Pulchowk, Lalitpur, Nepal
072bct527@ioe.edu.np

Aman Shakya
Institute of Engineering,
Tribhuvan University
Pulchowk, Lalitpur, Nepal
aman.shakya@ioe.edu.np

Sanjeeb Prasad Panday
Institute of Engineering,
Tribhuvan University
Pulchowk, Lalitpur, Nepal
sanjeeb@ioe.edu.np

ABSTRACT

This paper explores the application of deep learning techniques in the task of assessing disaster impact from satellite imagery. Identifying the regions impacted by a disaster is critical for effective mobilization of relief efforts. Satellite images, with their vast coverage of ground surface, are a valuable resource that can be leveraged for this purpose. However, the task of analysing a satellite image to detect regions impacted by disaster is challenging. In recent years, the increasing availability of satellite images of a place presents an opportunity to utilize deep learning on these images to provide a preliminary insight on the impact of a disaster after its occurrence. We particularly focus on water related disasters like floods and hurricanes. To identify the impacted regions, we employ Convolutional Neural Networks to semantically segment topographical features like roads on pre and post-disaster satellite images and find the regions with maximal change. However, this approach is less applicable on rural landscapes due to the sparse distribution of topographical features like roads. To address such cases of imagery from rural areas, we propose a bitemporal image classification approach to compare pre and post disaster scenes and directly identify if the regions are impacted or not. On testing against a ground truth satellite image from DigitalGlobe with labeled regions depicting the impacts of Hurricane Harvey, the flooded road extraction approach achieved an accuracy of 0.845 with a F1-Score of 0.675. Similarly, the bitemporal image classification approach registered an accuracy of 0.94 when tested against a rural landscape impacted by South Asian Monsoon Flooding of 2017.

© 2020 Association for Computing Machinery. ACM acknowledges that this contribution was authored or co-authored by an employee, contractor or affiliate of a national government. As such, the Government retains a nonexclusive, royalty-free right to publish or reproduce this article, or to allow others to do so, for Government purposes only.

IVSP 2020, March 20–22, 2020, Singapore, Singapore

© 2020 Association for Computing Machinery.

ACM ISBN 978-1-4503-7695-2/20/03...\$15.00

DOI: <https://doi.org/10.1145/3388818.3389160>

CCS Concepts

• Computing methodologies → Artificial intelligence → Computer vision → Computer vision problems → Image segmentation • Computing methodologies → Artificial intelligence → Computer vision → Computer vision tasks → Scene understanding • Computing methodologies → Machine learning → Machine learning approaches → Neural networks

Keywords

Disaster Assessment; Satellite Imagery; Deep Learning; Semantic Segmentation; Bitemporal Classification.

1. INTRODUCTION

Disasters typically occur suddenly causing economic damage, ecological disruption and loss of human life. In the advent of natural disasters, we need to prioritize relief efforts by identifying the regions which have been impacted the most. Extracting such critical information through on-site field surveys can take days or even weeks. At such times, satellite images are a valuable information source due to their vast ground coverage and increasing frequency of availability. One such work was done during the Nepal Earthquake of 2015 where ORCHID project in collaboration with Rescue Global used satellite imagery to map settlements across the affected areas for prioritized rescue [1]. However, the task of manually assessing and mapping the disaster impact is a tedious and time consuming task. With recent developments in computing methodologies and AI algorithms for object detection and scene identification, leveraging such ideas to speed up disaster response and management is a big necessity. This paper presents an effort made in that direction using deep learning on satellite imagery.

2. RELATED WORK

[2] and [3] document various efforts made in the past to use satellite imagery in mapping disaster impact and conducting relief efforts. [2] also reports that it requires 6 to 8 hours to manually map the disasters after the availability of satellite images. [4] presents an effort made to reduce the time cost of disaster assessment where the authors use Machine Learning and Computer Vision on remote sensing imagery to speed up the assessment of buildings damaged by the wildfires in California in 2017. In [5], the authors address a

similar issue by presenting a semi-supervised learning framework for large-scale damage detection in satellite imagery. They claim that their damage detection classifier results in a tenfold reduction in human annotation time at a minimal loss in detection accuracy. Although the initial efforts in utilizing satellite imagery for disaster assessment revolved largely around sensor-based technologies [6] [7], recent works have been harnessing the power of deep learning on scene understanding, image classification, image segmentation, etc and using them on satellite images. [8] and [9] deal with satellite imagery obtained after a disaster has occurred and apply Convolutional Neural Network (CNN) based approach to identify the damage due to the disaster. [8] primarily focuses on identifying flooded regions while [9] classifies buildings as damaged or not. A more comprehensive assessment of damage can be made by making a temporal comparison of images of a place before and after a disaster has occurred. [10] demonstrates such an approach employing a CNN based architecture to build an automated disaster detection system, especially for floods and landslides where they trained an image classifier that inputs both the pre and post images together. Another work that deals with assessing earthquake induced damage in buildings [11] reports that spatial features of texture and structure were far more important in algorithmic classification than spectral information. The work discussed above, however, requires a training corpus containing the images of disaster affected regions which is rare. Disasters like floods and hurricanes cause significant changes in the topographical features of the surface like submerging of road networks. Detecting changes in such features in pre and post disaster satellite imagery can help estimate the damage induced by the disaster in a region. Such a task would only rely on extracting topographical features from satellite imagery thus alleviating the need for disaster affected scenes in the training corpus. Authors of [12] have followed a similar approach where they use a Residual Inception Skip Network [13] to segment features like roads and buildings and quantify the differences in such features before and after a disaster.

In this paper, we build up on the previous works and use a Fully Convolutional semantic segmentation architecture: U-net [14] to extract the road networks in the satellite image of places before and after disasters like floods and hurricanes. The difference in the detected feature in the two images is then used to identify regions with maximal damage. Such an approach isn't suitable in rural landscapes with sparsely distributed road networks. So, we further build up on our approach by following a bitemporal image classification scheme where the pre and post disaster images are fed into a CNN to directly classify a region as flooded or not. In this regard, our contribution also lies in the preparation of a new dataset targeted for flooding identification in rural landscapes.

3. OVERVIEW OF PROPOSED APPROACH

Our main objective is to identify the regions most impacted by water related disasters like floods and hurricanes and map them on the available satellite imagery. For this, the problem is initially formulated to one of two types: (i) Mapping the impacted regions in an urban landscape with densely packed road networks. (ii) Mapping the impacted regions in a rural landscape with sparsely distributed road networks.

In (i), A road segmentation neural network is used to predict a binary segmentation mask of the pre and post disaster satellite images where each pixel get classified as belonging to a road or not. These segmentation masks are then fed into a change detection system which performs post processing operations like pixelwise

differencing and morphological opening for denoising. The change is then quantified to identify the impacted regions which are highlighted over the satellite image. This road extraction based method is invariant to lighting conditions and can be generalized to different types of urban landscapes.

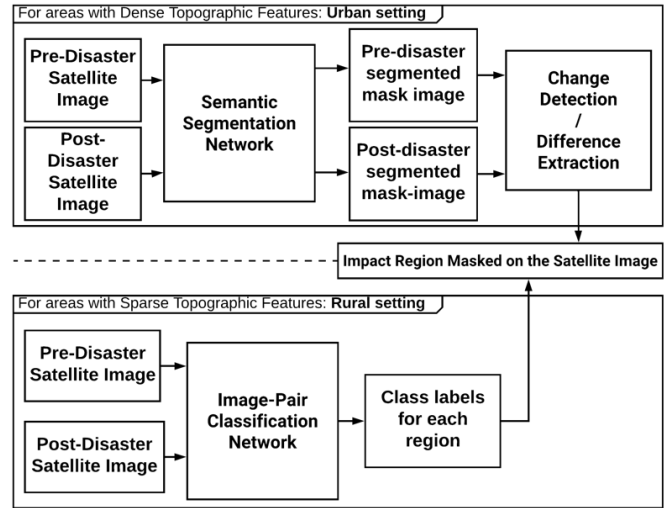


Figure 1. Block diagram demonstrating our approach

In (ii), the fact that the impact of floods in rural setting is seen mostly as inundated fields and eroded land cover rather than submerged roads is addressed. It is a more direct approach to disaster assessment compared to (i) as a bitemporal image classification scheme is used to directly identify flooded regions. Pre and post disaster satellite images are fed into the CNN network and the regions that are classified as flooded are further processed by our road extraction network in an attempt to discover any vital rural road networks that might have gone missing due to the flooding. Finally, the impacted regions are highlighted over the satellite image for manual inspection.

4. DATASETS

The datasets that are used in this research are detailed below:

4.1 For Road Extraction Based Approach

To assess the disaster impact in the urban areas with the approach discussed above, first, a semantic segmentation network is needed to generate binary masks indicating the roads from input satellite images. To train the neural network, the publicly available Deepglobe CVPR - Road Extraction Challenge Dataset [15] is used. It consists of satellite images at 50 cm resolution collected from DigitalGlobe satellites. Each image is of size 1024x1024 px and is paired with a grayscale mask image for road labels. The dataset is split into a training set consisting of 6,226 images and a test set of 1,243 images and augmentation is performed to increase the size of the dataset to prevent overfitting.



Figure 2. An RGB image and mask pair from the dataset

4.2 For Bitemporal Image Classification

This approach is designed to assess disaster impact on satellite images from rural landscapes. Due to the lack of publicly available dataset that fit our purposes, a new dataset was created by collecting the satellite images of regions from Nepal, India and Bangladesh that were affected by the Monsoon flooding of 2017. Each image is of size 256x256 px and were taken from the GeoTIFFs provided on the DigitalGlobe’s (now Maxar) OpenData platform [16]. The images in this custom dataset are given one of the 4 labels: (i) Not Flooded, (ii) Partially Flooded, (iii) Severely Flooded and (iv) Indecisive or obscured, as shown in Fig. 3. The dataset is split into a training set consisting of 15,505 such images and a test set consisting of 2,116 such images.

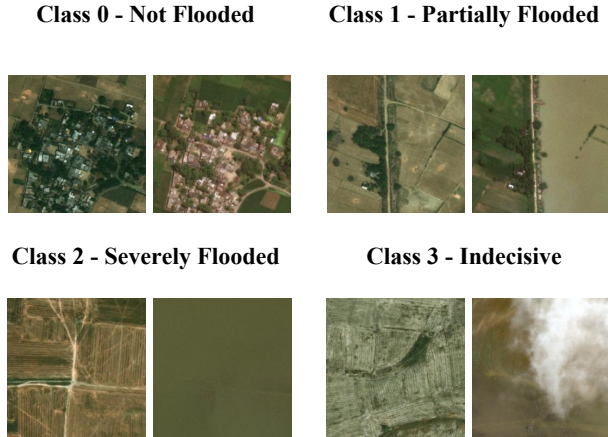


Figure 3. Examples of images from each class in the bitemporal image classification dataset

5. METHODOLOGY

This section describes in detail the approach taken to develop a disaster impact assessment system using the approach proposed in section 2.

5.1 Road Extraction Based Approach

The main tasks involved in designing a system to assess the damage caused by floods and hurricanes in an urban setting, with densely distributed road networks, can be divided into 4 phases: Data Preparation, Model Training, Difference Extraction and Impact Analysis.

5.1.1 Data Preparation

As discussed in section 4.1, the semantic segmentation neural network is trained using a pair of RGB satellite image and its corresponding mask labeling the road networks. For the model to generalize across a variety of scenes and prevent overfitting, a series of data augmentation routines like horizontal and vertical flips and random rotation is applied.

In majority of the mask images, the number of white pixels that belong to a road is far less in comparison to the black background pixels. This presents a class imbalance problem. This is addressed by weighing the positive examples (road pixels) in the Binary Cross Entropy loss function to increase the recall of the segmentation model.

$$weight = \frac{Total\ count\ of\ negative\ pixels}{Total\ count\ of\ positive\ pixels} \approx 22$$

5.1.2 Model Training

The data prepared for the training phase is used to train two variants of the famous semantic segmentation neural network: U-Net [14] which is a buildup on the Fully Convolutional Network [17]. It has an encoder portion that contracts the input image into a latent representation by repeated 3x3 convolution operations, each followed by ReLU and max pooling operation for downsampling. The next portion is the decoder which consists of a series of deconvolution or transposed convolution operation to upsample to the desired size of the image. The final output is a pixel-wise segmentation mask. In our task, the original U-Net architecture is modified into two separate variants and two experiments are conducted: (a) By decreasing the number of input filters to 16 to create a less parameterized version of U-Net which we call the *Parameterized U-Net* and (b) By replacing the original encoder CNN block with a ResNet-101 [18] network. When using the original U-Net architecture, the predictions tend to lack fine detail. To address this, cross or skip connections are added between blocks of the network which is done by ResNet. The loss function used in both variants is a linear combination of dice loss and a Binary Cross Entropy loss function. Also, dropout is applied for regularization and batch normalization is applied after all convolutional layers to ensure speed and stability in training the neural network. Both architectures are trained on NVIDIA Tesla T4 GPU provided by Google Colab. The following table summarizes the training setup for both the architectures discussed above:

Table 1. Training setup for road extraction

Architecture	Parameterized U-Net	U-Net with ResNet encoder
Number of Filters in the 1st Conv Layer	16	32
Dropout Regularization	0.1	0.2
Loss Function	Soft Dice + Binary Cross Entropy	Soft Dice + Binary Cross Entropy
Optimizer	Adam	Adam
Initial learning rate	0.001	0.005
Learning rate Scheduling	Manual scheduling	Manual scheduling
Activation Function	ReLU	ReLU
Mini Batch Size	8	12
Total Epochs trained	50	73

5.1.3 Difference Extraction

The binary segmentation masks of pre and post disaster images are generated by the semantic segmentation network. On these two masks, individually, morphological closing is performed followed by morphological opening in a successive fashion. Then the pixel-wise differencing of the two masks is performed. The difference image is further denoised by a morphological opening operation.

All morphological operations are carried out using a rectangular kernel of size 3x3 as the structuring element.

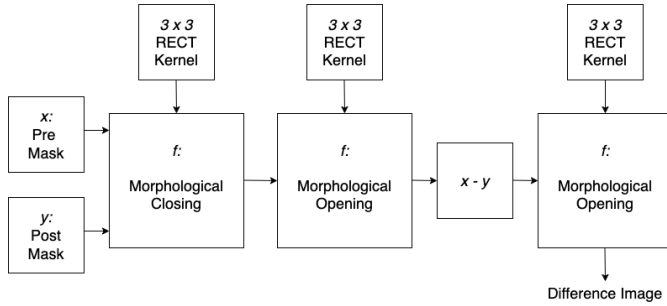


Figure 4. Flow diagram for the difference extraction process

5.1.4 Impact Analysis

The difference image indicates the roads that have been inundated and are missing after the flood. A 256x256 px box defines a region in the difference image and a criteria is defined to categorize any observed region as impacted or not. It examines the amount of roads that are missing in a region of the post disaster image mask compared to the same region in the pre disaster image mask. The impacted regions are those which satisfy:

$$\frac{\text{No. of non zero pixels in difference image}}{\text{No. of non zero pixels in pre mask}} > \text{threshold}$$

Here, *threshold* is an empirically chosen constant (typically 0.4 or 0.5).

A 256x256 px window is slid across the entire difference image and if the region falling inside the window satisfies the above criteria, it is marked as impacted. As an approach for fine tuning, another sliding window of size 64x64 px is run in the neighborhood of the impacted regions and those regions that satisfy the above criteria are classified as impacted.

5.2 Bitemporal Image Classification

The main tasks involved in designing a system to assess the damage caused by floods and hurricanes in a rural setting, with sparsely distributed road networks, can be divided into 3 phases: Data Preparation, Model Training and Highlighting Missing Roads (if any).

5.2.1 Data Preparation

The images in the dataset described in section 4.2 was validated for its correctness by experts in flood rescue and relief operations at UNDP, Nepal. Similar to 5.1.1, augmentation techniques like horizontal and vertical flips are applied along with random rotation to generalize the model across multiple settings. The RGB channels in each image are normalized using the mean and standard deviation of the ImageNet dataset.

$$X = \frac{X - \text{Mean}}{\text{Std. Deviation}}$$

Here, Mean = [0.485, 0.456, 0.406] and Standard Deviation = [0.229, 0.224, 0.225] for channels [Red, Green, Blue] respectively.

5.2.2 Model Training

The data prepared by 5.2.1 is used to train two state-of-the-art neural networks for image classification and their performance in assessing the disaster impact in rural landscape is compared. (Discussed further in 6.2). The two networks are: (a) ResNet-50 which is a 50 layer deep residual neural network [18] and utilizes skip connections in its architecture to address the vanishing gradient problem allowing the network architecture to have deep

layers. (b) ResNeXt-50 [19] which is a highly modularized, multi-branched variant of the ResNet architecture.

Since, the task is a bitemporal image classification, the network needs to make the prediction by analysing the image of the place at two different points of time (before and after the disaster). Hence, both the pre and post disaster satellite images are stacked along the channel dimension to form a 6 channel input image. Here, the first 3 channels are the RGB channels from the pre disaster image and the last 3 channels are the RGB channels from the post disaster image. To accommodate the neural network for classifying such an image, the first layer of both (a) and (b) are modified to input 6 channels instead of 3. Also, the final layer in the standard architectures of (a) and (b) is replaced with a softmax activation layer consisting of 4 neurons, one for each output class.

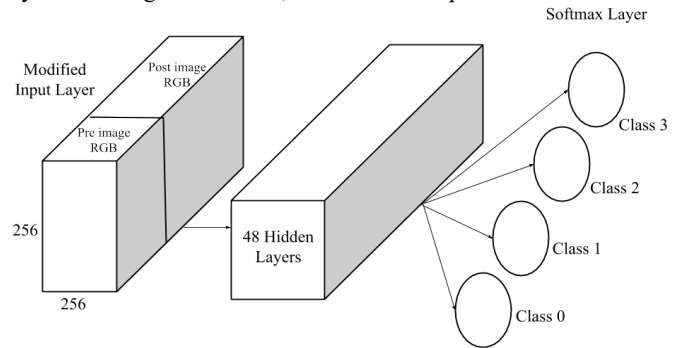


Figure 5. Modification of ResNet and ResNeXt architectures for bitemporal image classification

While experimenting with both (a) and (b), the network weights are initialized using the pretrained weights for ImageNet dataset. Also, dropout is used for regularization and Categorical Cross Entropy is used as the loss function to train the network. Both architectures are trained on NVIDIA Tesla T4 GPU provided by Google Colab. The following table summarizes the training setup for both the architectures discussed above:

Table 2. Training setup for bitemporal image classification

Architecture	ResNet-50	ResNeXt-50
Network Depth	50	50
Dropout Regularization	0.4	0.4
Loss Function	CCE	CCE
Optimizer	Adam	Adam
Initial learning rate	0.001	0.001
Learning rate scheduling	Manual scheduling	Manual scheduling
Activation Function	ReLU	ReLU
Mini Batch Size	64	64
Epochs Trained	50	50

5.2.3 Highlighting Missing Roads

The satellite image of the rural area is divided into grids of 256x256 px. Each such grid defines a region in the image and is fed into the classifier to generate the prediction. After receiving the predictions for each region, the partially and severely flooded regions are highlighted as the regions impacted by the disaster. In some rural areas, floods might submerge few vital road networks which are often the only routes for rescue and relief operations by land. As an effort to provide such additional insight, only the impacted regions from the rural satellite image are selected and checked if any important road networks have been submerged by inputting them into our already trained road extraction network. Along with the highlighting of impacted regions, the mapping of missing roads (if any) can help the relief workers to plan relief and rescue routes effectively.

6. RESULTS

This section details the findings and results of the experiments that were carried out following the procedure described in section 5.

6.1 Road Extraction Based Approach

First, an experiment to assess the disaster impact in an urban setting was carried out for which the approach discussed in 5.1 was followed.

As the preliminary step for this experiment, the performance of the two semantic segmentation neural networks (see 5.1.2) in the road extraction task was evaluated against the test dataset discussed in 4.1. Between Parameterized U-Net and U-Net with ResNet encoder, the latter was seen to have better performance in this task.

Table 3. Road segmentation IoU score for training and test sets of section 3.1

Architecture	Parameterized U-Net	U-Net with ResNet encoder
Train set IoU	0.72	0.83
Test set IoU	0.67	0.68

After obtaining satisfactory performance from the road segmentation networks, the next step of the experiment was carried out, i.e. identifying the disaster impacted regions by performing the difference extraction and impact analysis techniques described in 5.1.3 and 5.1.4.

Here, the performance of our proposed approach was evaluated in the task of identifying the regions of Southeast Texas impacted by the Hurricane Harvey disaster of 2017. For this, the pre and post disaster image of the area along with its corresponding ground truth labels for the impacted regions was obtained from the authors of [12]. The pre and post disaster satellite images were then input to the semantic segmentation neural network which predicted their corresponding road masks. Performing the operations of 5.1.3 and 5.1.4 on the pre and post disaster road segmentation masks, the regions impacted by the hurricane was predicted and the results were compared with the corresponding ground truth using standard evaluation metrics:

Table 4. Performance of the disaster assessment system in identifying the regions impacted by Hurricane Harvey using Parameterized U-Net for road extraction

Evaluation Metric	Score
IoU	0.372
Accuracy	0.665
Precision	0.486
Recall	0.614
F1 Score	0.543

Evaluation Metric	Score
IoU	0.512
Accuracy	0.845
Precision	0.526
Recall	0.956
F1 Score	0.677

Table 5. Performance of the disaster assessment system in identifying the regions impacted by Hurricane Harvey using U-Net with ResNet encoder for road extraction

Evaluation Metric	Score
IoU	0.372
Accuracy	0.665
Precision	0.486
Recall	0.614
F1 Score	0.543

It can be seen from the tables 4 and 5 that the approach using U-Net with ResNet encoder outperforms the approach using Parameterized U-Net. Hence, U-Net with ResNet encoder was chosen as the preferred network for road extraction in the disaster assessment system.

The following figure shows an example of the output provided by our system when the images before and after Hurricane Harvey were provided as input.

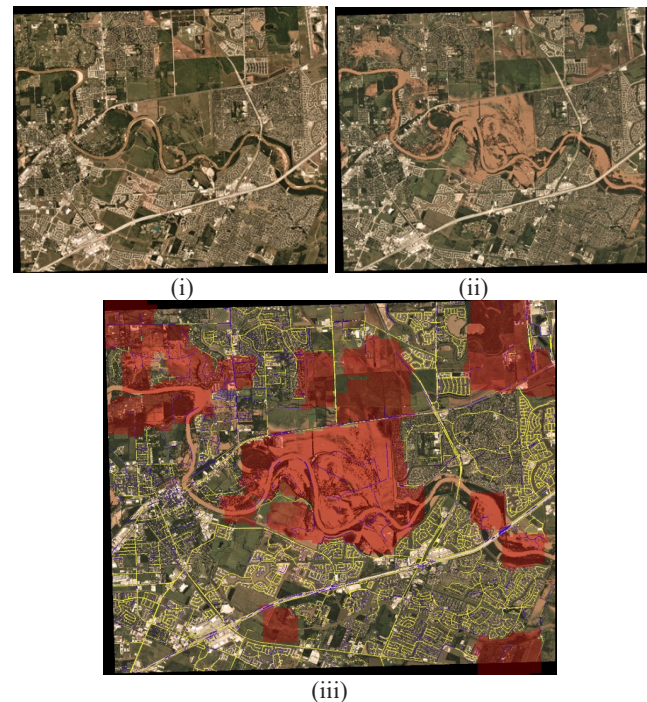


Figure 5. Satellite imagery of Southeast Texas (i) before (ii) after (iii) with impacted regions highlighted. Blue lines indicate inundated roads

6.2 Bitemporal Image Classification

Second, an experiment was carried out to assess the disaster impact in a rural setting for which the approach discussed in 5.2 was followed.

The performance of this approach was evaluated in the task of classifying the regions of Gorakhpur area (near the Nepal-India border) impacted by the monsoon flooding of 2017. This was obtained from the test dataset described in section 4.2 and annotated by experts from UNDP Nepal. Separate experiments were performed with ResNet-50 and ResNeXt-50 (see section 5.2.2) as the classifier of our disaster assessment system and their predictions for impacted regions were compared against the ground truth labels using standard evaluation metrics.

The overall accuracy of the system using ResNet-50 as the classifier was 93.76% whereas using ResNeXt-50 as the classifier gave an accuracy of 94.75%. The following tables document the class-wise evaluation metrics for both instances of the experiment:

Table 6. Performance of the disaster assessment system in classifying the regions impacted by monsoon flooding using ResNet-50 as the bitemporal image classifier

Class	Precision	Recall	F1-Score
Not Flooded (0)	0.9757	0.9484	0.9619
Partially Flooded (1)	0.7535	0.8023	0.7771
Severely Flooded (2)	0.9577	0.9624	0.9600
Indecisive (3)	0.95	0.9779	0.9637

Table 7. Performance of the disaster assessment system in classifying the regions impacted by monsoon flooding using ResNeXt-50 as the bitemporal image classifier

Class	Precision	Recall	F1-Score
Not Flooded (0)	0.9719	0.9697	0.9798
Partially Flooded (1)	0.7793	0.8593	0.8173
Severely Flooded (2)	0.9763	0.9515	0.9637
Indecisive (3)	0.9772	0.9485	0.9626

The results show that ResNeXt-50 performs better as the bitemporal image classifier for classifying regions impacted by flood in a rural setting and was therefore chosen over its ResNet-50 counterpart in our disaster assessment system. The following figure shows an example of the output provided by our system when the images before and after the monsoon flooding were provided as input:

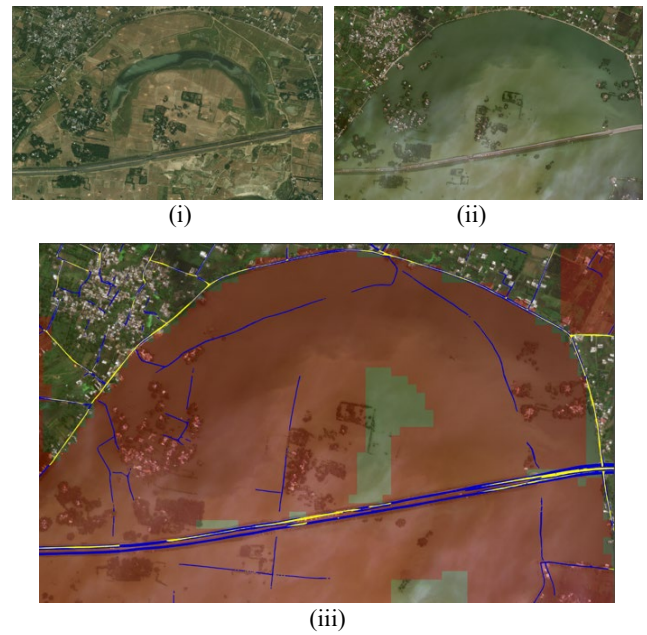


Figure 6. (i) Satellite imagery of Gorakhpur region before monsoon flooding. (ii) Satellite imagery of Gorakhpur region after monsoon flooding. (iii) Satellite imagery of Gorakhpur region with impacted regions highlighted. The missing roads present are indicated by blue lines.

7. CONCLUSION & FUTURE WORK

In this paper, an approach is presented to assess the impact caused by water related disasters like floods and hurricanes in urban as well as rural landscapes. To identify the impacted regions in an urban landscape, the changes in the road networks before and after the disaster are monitored and the change is quantified as impact. For this, a semantic segmentation neural network called U-Net is used with ResNet encoder that was trained on a road segmentation dataset to extract the roads in both the pre and post disaster images. The two segmentation masks thus obtained are then processed by a pipeline involving morphological denoising and differencing operations. Finally, the difference is quantified as impacts and the impacted regions are overlaid on the satellite image. To address the fact that rural landscapes lack enough road networks and the impact of floods in such settings is seen as inundation of fields and land cover, a different approach is adopted to assess the disaster impact. The images of a place from two different time points (before and after the disaster) are stacked together to form a composite image that is then fed into a bitemporal image classifier based on a residual CNN architecture called ResNeXt-50. The severity of the impact caused by the disaster in that region is then directly predicted by the classifier. The developed system has been tested on areas affected by Hurricane Harvey and South Asian Monsoon Flooding and has been deployed at <http://manaslu.pcampus.edu.np/disaster/> as a web application featuring OpenStreetMap integration and map-based navigation.

Currently, the system only analyses the change in road networks but other topographical features like the buildings and land cover can also be considered to generalize the system to non-water related disasters like earthquakes and wildfires. Similarly, as of now, the pre and post disaster images that the system takes as input need to be properly registered and aligned with each other. Efforts in making the system robust to misalignment can be explored in the future. Motivation for this can be taken from [20] which proposes an object based change detection technique. Another interesting

research direction could be automatically identifying a region as belonging to urban or rural landscape increasing the level of autonomy in the system and providing greater assistance to the relief workers who use this system to assess the disaster impacts.

8. ACKNOWLEDGMENTS

This project has been supported by the University Grants Commission, Nepal under a Collaborative Research Grant (UGC Award No. CRG-74/75-Engg-01). Our gratitude also goes to UNDP Nepal for helping us with data annotation.

9. REFERENCES

- [1] Orchid. 2015. ORCHID researchers provide Nepal earthquake response. Retrieved from: <http://www.orchid.ac.uk/presses/orchid-researchers-provide-nepal-earthquake-response/>
- [2] Voigt, S., Giulio, F. T., et al. 2016. Global trends in satellite-based emergency mapping. *Science*. 353. 247-252. DOI: <https://dx.doi.org/10.1126/science.aad8728>
- [3] Voigt, S., Kemper, T., Riedlinger, T., Kiefl, R., Scholte, K. and Mehl, H. 2007. Satellite Image Analysis for Disaster and Crisis-Management Support. *IEEE T. Geoscience and Remote Sensing*. 45. 1520-1528. DOI: <https://dx.doi.org/10.1109/TGRS.2007.895830>
- [4] Trekin, A., Novikov, G., Potapov, G., Ignatiev, V. and Burnaev, E. 2018. Satellite Imagery Analysis for Operational Damage Assessment in Emergency Situations. arXiv:1803.00397. Retrieved from: <https://arxiv.org/abs/1803.00397>
- [5] Gueguen, L. and Hamid, R. 2015. Large-Scale Damage Detection Using Satellite Imagery. In *Proceedings of the IEEE Conference on Computer Vision and Pattern Recognition* (Boston, MA, USA, June 07-12, 2017). IEEE. 1321-1328. DOI: <https://dx.doi.org/10.1109/CVPR.2015.7298737>
- [6] Matikainen, L., Juha, H., Kaartinen, H., et al. 2004. Automatic detection of changes from laser scanner and aerial image data for updating building maps, *Matrix*, 35, 434-439.
- [7] Vu, T. T., Matsuoka, M. and Yamazaki, F. 2004. LIDAR-based Change Detection of Buildings in Dense Urban Areas. In *Proceedings of the IEEE International Geoscience and Remote Sensing Symposium* (Anchorage, AK, USA, September 20-24, 2004). IEEE. 2-6. DOI: <https://dx.doi.org/10.1109/IGARSS.2004.1370438>
- [8] Nogueira, K., Fadel, S., Dourado, I., Werneck, R., et al. 2017. Exploiting ConvNet Diversity for Flooding Identification. *IEEE Geoscience and Remote Sensing Letters*. 15. 1446-1450. DOI: <https://dx.doi.org/10.1109/LGRS.2018.2845549>
- [9] Cao, Q. D. and Choe, Y. 2018. Building Damage Annotation on Post-Hurricane Satellite Imagery Based on Convolutional Neural Networks. arXiv: 1807.01688. Retrieved from: <https://arxiv.org/abs/1807.01688>
- [10] Binti, A., Siti, N. K. and Aoki, Y. 2017. Disaster detection from aerial imagery with convolutional neural network. *International Electronics Symposium on Knowledge Creation and Intelligent Computing* (Surabaya, Indonesia, September 26-27, 2017). 239-245. DOI: <https://dx.doi.org/10.1109/KCIC.2017.8228593>
- [11] Cooner, A. J., Shao, Y. and Campbell, J. B. 2016. Detection of Urban Damage Using Remote Sensing and Machine Learning Algorithms: Revisiting the 2010 Haiti Earthquake. *Remote Sensing*. 8, 868. DOI: <https://doi.org/10.3390/rs8100868>
- [12] Doshi, J., Basu, S. and Pang, G. 2018. From Satellite Imagery to Disaster Insights. arXiv: 1812.07033. Retrieved from: <https://arxiv.org/abs/1812.07033>
- [13] Doshi, J. 2018. Residual inception skip network for binary segmentation. In *Proceedings of the IEEE Conference on Computer Vision and Pattern Recognition Workshops* (Salt Lake City, UT, USA, June 18-22, 2018). IEEE. 216-219 DOI: <https://doi.org/10.1109/CVPRW.2018.00037>
- [14] Ronneberger, O., Fischer, P. and Brox, T. U-Net: Convolutional Networks for Biomedical Image Segmentation. arXiv: 1505.04597. Retrieved from: <https://arxiv.org/abs/1505.04597>
- [15] Demir, I., Koperski, K., Lindenbaum, D., et al. 2018. DeepGlobe 2018: A Challenge to Parse the Earth through Satellite Images. arXiv:1805.06561. Retrieved from: <https://arxiv.org/abs/1805.06561>
- [16] DeepGlobe Open Data Program. Retrieved from: <https://www.digitalglobe.com/ecosystem/open-data>
- [17] Schelhamer, E., Long, J. and Darrel, T. 2016. Fully Convolutional Networks for Semantic Segmentation. *IEEE Transactions on Pattern Analysis and Machine Intelligence*. 39. 640-651. DOI: <https://doi.org/10.1109/TPAMI.2016.2572683>
- [18] He, K., Zhang, X., Ren, S. and Sun, J. 2015. Deep Residual Learning for Image Recognition. arXiv:1512.03385. Retrieved from: <https://arxiv.org/abs/1512.03385>
- [19] Xie, S., Girshick, R., Dollar, P., Tu, D. and He, K. Aggregated Residual Transformations for Deep Neural Networks. arXiv:1611.05431. Retrieved from: <https://arxiv.org/abs/1611.05431>
- [20] Bukenya, F., Yuhaziz, S., Hashim, S. Z. M. and Kalema, A. K. 2012. Detecting floods using an object based change detection approach. *International Conference on Computer and Communication Engineering* (Kuala Lumpur, Malaysia, July 3-5, 2012). IEEE. DOI: <https://doi.org/10.1109/ICCCE.2012.6271149>